Journal of Materials and Electronic Devices 5 (2023) 35-41

JOURNAL OF MATERIALS AND ELECTRONIC DEVICES
FYTRONIX JMED http://dergi-fytronix.com/

Investigation of capacitance and conductance characteristics of pyrene-based Schiff base Schottky diode prepared by spin coating method

Enis Taşcı[1,*]

[1]Vocational High School of Health Services, Giresun University, Giresun, Turkiye

This study aimed to produce an Al/PyMIs/n-Si/Al Schottky diode utilizing isoniazid and pyrene-based Schiff base (PyrMIs) thin film on n-type Si. Thin film was deposited by spin coating. The Al/PyMIs/n-Si/Al diode's capacitance (*C*) and conductance (*G*) were measured at various frequencies and voltages. A voltage range of (-2V) to (+2V) and a frequency range of 1 kHz to 1 MHz were used for testing the diode. The series resistance (R_s) and interface state density (N_{ss}) values were determined using the conductance and Hill-Coleman methods, in that order, in accordance with the frequency. At 2V, the series resistance values decreased from 1.07 kΩ to 33.8 Ω over the 1 kHz and 1 MHz frequency ranges, respectively. The interface state density was calculated to be within the range of 10^{12} eV^{-1} cm^{-2}.

Keywords: *Pyrene, Schiff base, Schottky diode, series resistance, interface state density*

Submission Date: 17 October 2023
Acceptance Date: 08 December 2023

**Corresponding author:* enistasci@giresun.edu.tr

1. Introduction

The electrical characteristics of Schottky barrier diodes (SBDs) of the metal-semiconductor (MS) and metal-interface layer-semiconductor (MIS) types have been the subject of extensive research for a long period of time [1-3], owing to their technological benefits in optoelectronic applications. The phenomenon of nonideal electrical behavior exhibited by SBDs has been commonly ascribed to the influence of properties of the interface layer [4, 5]. The interfacial layer development at the MS interface, the level of interface states (N_{ss}) at the organic layer/Si interface, and the series resistance (Rs) of the devices have a significant impact on the performance of these diodes. Consequently, determining the interface properties of a Schottky diode with an organic base is critical [6]. Furthermore, frequency-dependent C–V and G–V measurements across a broad frequency range can provide significant insights into the energy distribution of interface states and the structures in discussion [7]. Conversely, the capacitance-voltage (C-V) and conductance-voltage (G-V) characteristics of SBDs are significantly influenced by the series resistance R_s of the semiconductor bulk. As a result, the interface state density N_{ss} derived from admittance spectroscopy deviates from what was expected [8].

Organic materials are widely used in various electronic and optoelectronic devices like diodes, thin-film transistors, sensors, and solar cells. These organic materials, including organic molecules, organometallics, and polymer nanostructures, enhance the performance of these devices. Schiff bases, a popular organic semiconductor, offer an alternative to traditional conjugated compounds due to their ease of synthesis and isoelectronicity with vinyl analogs [6, 7].

This study examines the use of a pyrene-based Schiff base as an interlayer in MS structures. It investigates the properties of the Al/PyMIs/n-Si/Al diode under forward and reverse bias conditions, at various frequencies and applied bias voltage ranges. The study also examines the impact of the insulating layer, series resistance, and interface state density on the conductivity-voltage and capacity-voltage measurements of Schottky diode devices with a metal/organic material/semiconductor (MOmS) configuration. Conductivity-voltage and capacitance-voltage measurements are conducted across a broad frequency range (1 kHz–1000 kHz) in order to minimize the influence of interface states.

2. Experimental

2.1. Synthesis of PyMIs

The synthesis of PyMIs, prepared as the literature procedure, is depicted in Fig. 1. As seen, a simple one-step condensation reaction between the isoniazid (1) and pyrene-1-carbaldehyde (2) gives PyMIs in good yield. The structure was confirmed using ^{1}H and ^{13}C spectroscopy [9].

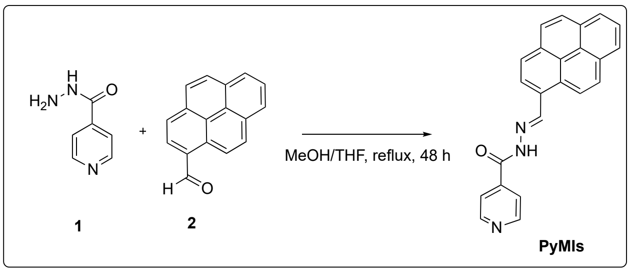

Figure 1: Synthetic route to PyMIs

2.2. Production of Al/PyMIs/n-Si/Al Diode

The n-type Si crystal was used for diode production, with an orientation of (100), a thickness of 500 µm, and a resistivity of 1-20 Ω-cm. The crystal was cleaned, etched, rinsed, and dried in nitrogen gas. The aluminum metal sub-contact was evaporated, and a solution of CHCl3:PyMIs was applied to the n-Si crystal. A rectifier contact was formed by thermally depositing 200 nm Al metal through a copper shadow mask. The MOmS Schottky type diode was produced, with a contact area of 4.335 x 10^{-2} cm^{2}. Schematic diagram of Al/PyMIs/n-Si/Al diode was illustrated in Fig 2. The diode's interface state density and series resistance characteristics were analyzed using conductance-voltage and capacitance-voltage measurements. A HP 4192A impedance analyzer was used to acquire admittance data from the device structure.

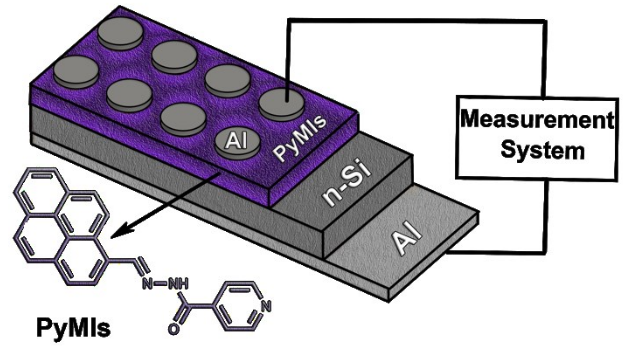

Figure 2: Schematic diagram of Al/PyMIs/n-Si/Al diode

3. Results

Capacitance-voltage (C-V) and conductance-voltage (G-V) measurements were taken to reveal the frequency-dependent series resistance and interfacial state density distributions of the produced device. These measurements were made in a broad measuring range of -2V- +2V and 1 kHz-1 MHz. The measured capacitance (C_m) of the diode is plotted in Figure 3 with varying voltage in the various frequencies (1 kHz – 1 MHz). Figure 3 depicts that the capacitance values are nearly independent of especially low frequency at inversion region. As we increase the frequency applied to the sample, the total capacitance of the diode is significantly affected by the bulk resistance and the capacitance of the depletion layer. The result is a capacitance dispersion associated with electron and hole flow from slow-response deep level impurity levels. Figure 3 clearly show that there are three regions of accumulation, depletion, and reversal, confirming typical metal-organic material interface-semiconductor (MOmS) behavior for each A.C. frequency. The measured conductance (G_m) of the diode is plotted in Figure 4 with varying voltage in the various frequencies (1 kHz – 1 MHz). The observed behavior in G_m-V plots at lower frequencies (f <100 kHz) can be refered by the interface traps and reordering of traps under an external electric field. Conductance values don't almost vary with increasing frequency in the negative voltage part. The movement of conductance with increasing frequency is due to the presence of surface state at the between organic layer and n-Si interface [1, 10, 11].

The device was characterized using capacitance-voltage (C-V) and conductance-voltage (G-V) measurements in order to determine the frequency-dependent distribution of series resistance and interfacial state density. The measurements were conducted within a wide range of -2V to +2V and from 1 kHz to 1 MHz. The diode's capacitance (C_m) was measured and shown in Figure 3, showing the changes in voltage across several frequencies ranging from 1 kHz to 1 MHz. Figure 3 illustrates that the capacitance values remain rather constant, particularly at low frequencies, within the inversion zone. The overall capacitance of the diode is greatly influenced by the bulk resistance and the capacitance of the depletion layer when we raise the frequency supplied to the sample. The outcome is a phenomenon of capacitance dispersion linked to the movement of electrons and holes from deep-level impurity levels with sluggish reaction. Figure 3 unambiguously demonstrates the presence of three distinct areas of accumulation, depletion, and inversion, thereby proving the characteristic metal-semiconductor (MS) behavior for each alternating current (A.C.) frequency. The diode's conductance (G_m) was measured and shown in Figure 4, showing the variation of voltage across several frequencies ranging from 1 kHz to 1 MHz. The value of capacitance decreases with frequency at all voltages. The pattern exhibited in G_m-V graphs at frequencies below 100 kHz can be attributed to the presence of interface traps and the rearrangement of traps in response to an external electric field. The conductance values exhibit minimal variation as the frequency increases in the negative voltage range. The variation in conductance as frequency increases is attributed to the existence of surface states at the interface between the organic layer and the n-Si [11, 12].

Figure 5 (a) and (b) show the capacitance-frequency (C_m-f) and conductance-frequency (G_m-f) graphs of the Al/PyMIs/n-Si/Al diode. The measurements were taken at voltages ranging from -2V to 2V, with increments of 0.5V, and at frequencies between 1 kHz and 1000 kHz. From Figure 5 (a), we noticed that the capacitance values exhibit a peak in the low-frequency range, decrease in the middle and high frequency range at the measured voltages. The conductance exhibited in Figure 5 (b) is in direct contrast to the capacitance observed in Figure 5 (a). At lower frequencies, the conductance value gradually increases as the frequency increases. In addition, Figure 5 (a) demonstrates that the diode generated exhibits a significant capacitance value exclusively at low frequencies, and possesses charge carriers capable of tracking the AC signal transmitted to the diode. At 0V, while the capacitance of the produced diode decreased from 5.37×10^{-9} F to 1.94×10^{-9} F, the conductance of the constructed diode increased from 3.62×10^{-6} S to 8.23×10^{-3} S as the frequency increased from 1 kHz to 1 MHz, respectively.

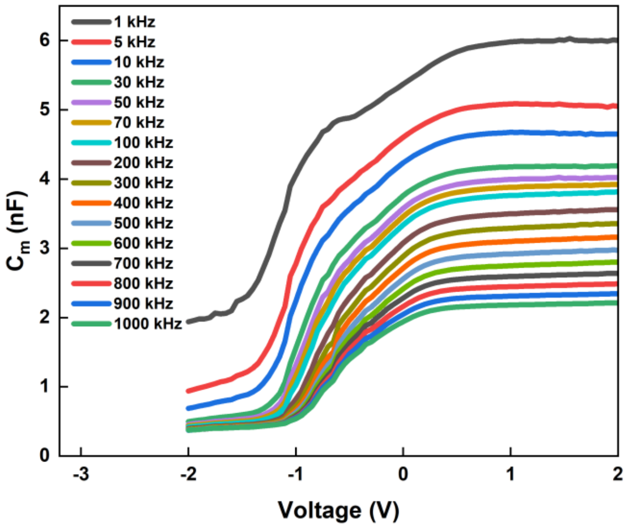

Figure 3: Plots of C_m-V of the Al/PyMIs/n-Si/Al diode in various frequencies 1 kHz-1 MHz.

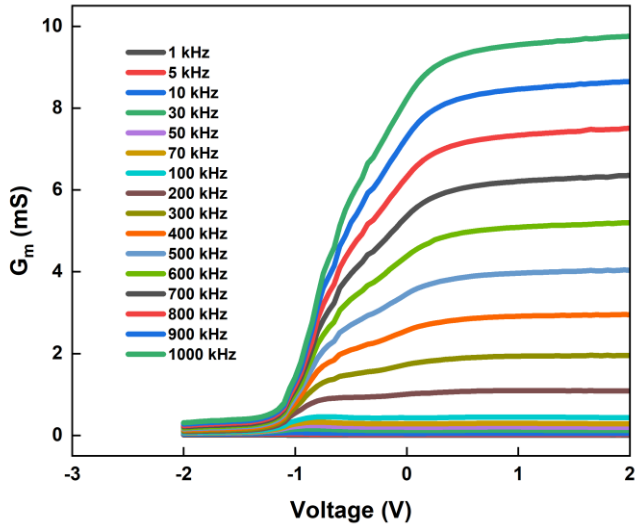

Figure 4: Plots of G_m-V of the Al/PyMIs/n-Si/Al diode in various frequencies 1 kHz-1 MHz.

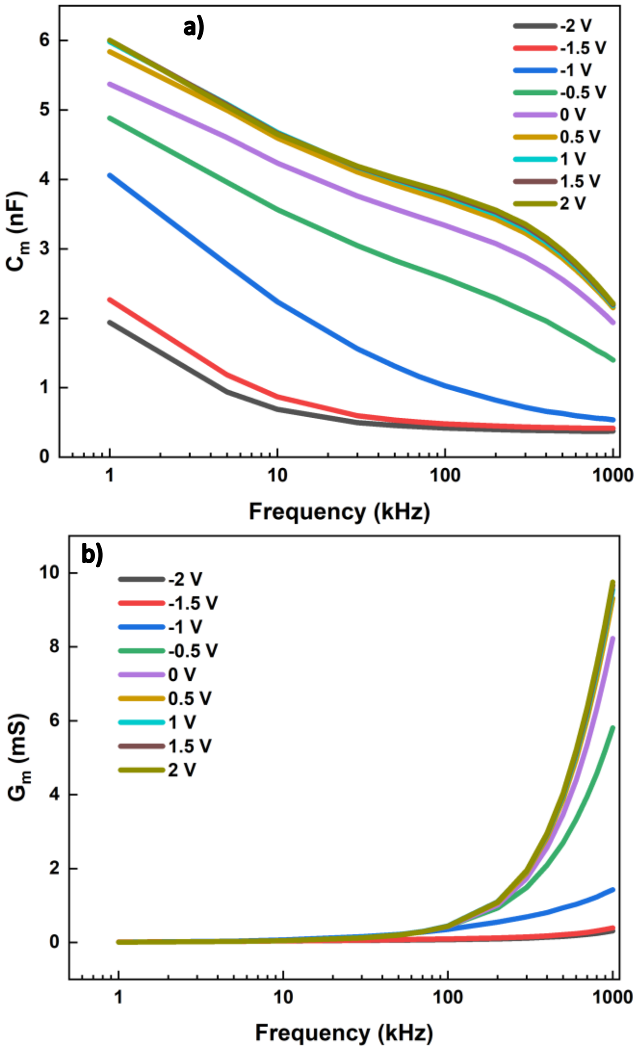

Figure 5: Plots of (a) C_m-*Logf* and (b) G_m-*Logf* of the Al/PyMIs/n-Si/Al diode in various voltages.

The existence of series resistance (R_s) results in the non-ideal behavior of the electrical characteristics of the diode. The calculation and impact of it must be deducted from the measured capacitance and conductance values. The Niccolian and Goetzberger technique can be used to calculate series resistance values [10, 13]:

$$R_s = \frac{G_m}{G_m^2 + (\omega C_m)^2} \quad (1)$$

Where C_m and G_m are the measured capacitance and conductance values at all frequency region, respectively.

Figure 6 displays the plotted series resistance (R_s) of the diode as a function of voltage across a range of frequencies (1 kHz-1 MHz). The series resistance levels fall as the frequencies increase, reaching their greatest value at negative voltages. Nevertheless, the values of series resistance decrease with increasing frequency. The series resistance values of the produced diode decreased from 55.6 Ω to 33.8 Ω as the voltage reached from -2V to 2V, respectively, at a frequency of 1 MHz.

Figure 7 illustrates the relationship between series resistance and frequency (R_s-*f*) for the Al/PyMIs/n-Si/Al Schottky diode. The voltage range tested was -2V to 2V, with increments of 0.5V. The frequencies ranged from 1 kHz to 1 MHz. Figure 7 demonstrates that the series resistance values decrease with higher frequencies and voltages. The series resistance of the produced diode decreased from 1.07 kΩ to 33.8 Ω as the frequency increased from 5 kHz to 1 MHz.

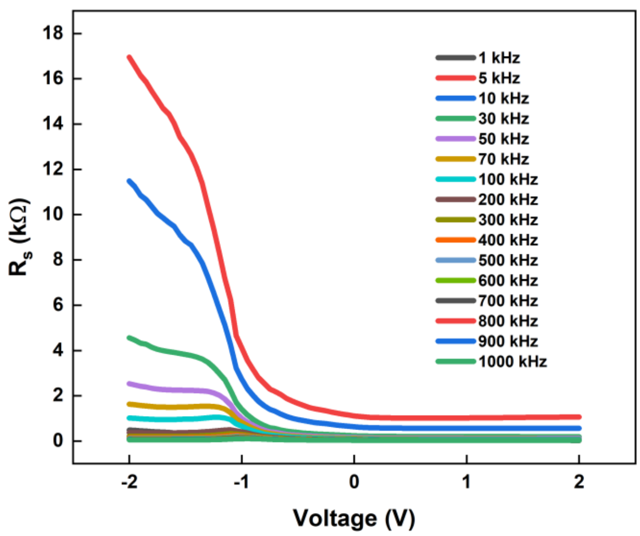

Figure 6: Plots of R_s-*V* of the Al/PyMIs/n-Si/Al diode in various frequencies.

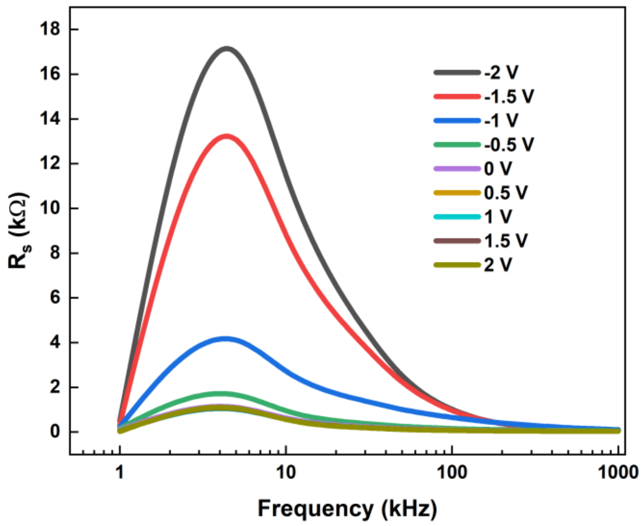

Figure 7: Plots of R_s-*Logf* of the Al/PyMIs/n-Si/Al diode in various voltages.

The measured *C* and *G* characteristics can be corrected to remove the effect of Rs in the inversion, depletion and accumulation regions using the following equations [1, 14-16]:

$$G_c = \frac{(G_m^2+\omega^2 C_m^2)a}{a^2+\omega^2 C_m^2} \quad (2)$$

$$C_c = \frac{(G_m^2+\omega^2 C_m^2)C_m}{a^2+\omega^2 C_m^2} \quad (3)$$

$$a = G_m - (G_m^2 + \omega^2 C_m^2)R_s \quad (4)$$

The corrected capacitance and conductance values across the entire frequency range are denoted as C_c and G_c, respectively. Figure 8 illustrates the relationship between voltage and the corrected capacitance C_c of the diode across a range of frequencies (1 kHz-1 MHz). The corrected capacitance values were greater than the measured capacitance values once the series resistance effect was eliminated. As an illustration, the values for C_m and C_c increased from 2.21×10^{-9} F to 3.30×10^{-9} F at 2V, respectively, when measured at 1 MHz. The G_c-V characteristics exhibit a peak in the depletion region across all frequencies, as depicted in Figure 9. Furthermore, the corrected G_c values demonstrate an upward trend with increasing frequency. In particular, these peaks migrate toward higher voltages as frequency increases. The existence of interfacial states is indicated by the presence of a peak at each frequency [1, 14-16].

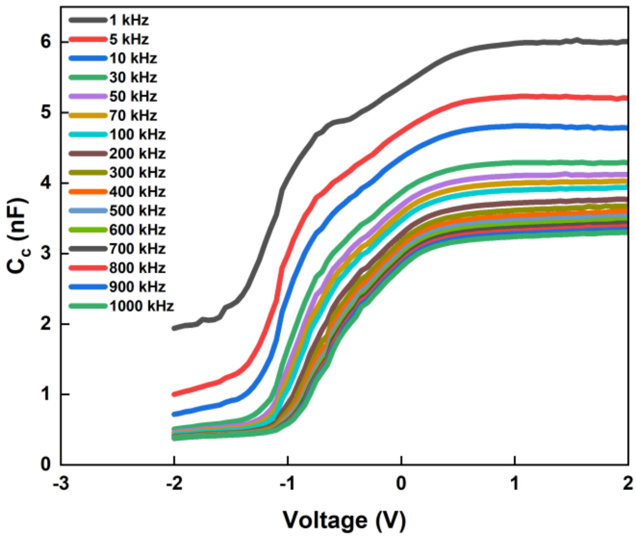

Figure 8: Plots of C_c-V of the Al/PyMIs/n-Si/Al diode in various frequencies 1 kHz-1 MHz.

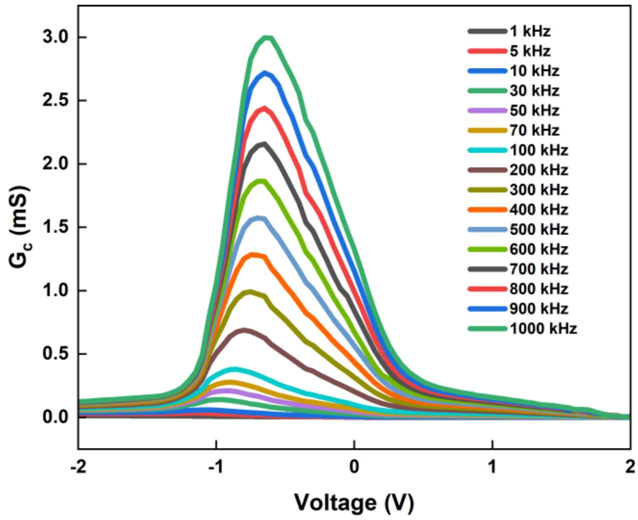

Figure 9: Plots of G_c-V of the Al/PyMIs/n-Si/Al diode in various frequencies 1 kHz-1 MHz.

The Hill-Coleman technique [17] is often used for calculating the interface state density (N_{ss}) value. The N_{ss} values of the diode can be determined as a function of frequency using the Hill-Coleman technique. This involves calculating the N_{ss} values based on the peak values of the conductance-voltage curves, using the equation provided [17, 18]:

$$N_{ss} = \frac{2(G_{c,max}/\omega)}{qA}\left[(1 - C_c/C_i)^2 + \left(G_{c,max}/\omega C_i\right)^2\right]^{-1} \quad (5)$$

The N_{ss} values were computed using equation 5, utilizing the corrected conductance peaks, and subsequently visualized in Figure 10. Figure 10 illustrates a clear inverse relationship between N_{ss} values and frequency, indicating that as the frequency increases, the N_{ss} values decrease. The loss in capacity is attributed to the inability of charge carriers to contribute at high frequencies [19]. The N_{ss} values were determined to be 1.78×10^{12} eV^{-1} cm^{-2} and 5.49×10^{11} eV^{-1} cm^{-2} at frequencies of 1 kHz and 1 MHz, respectively.

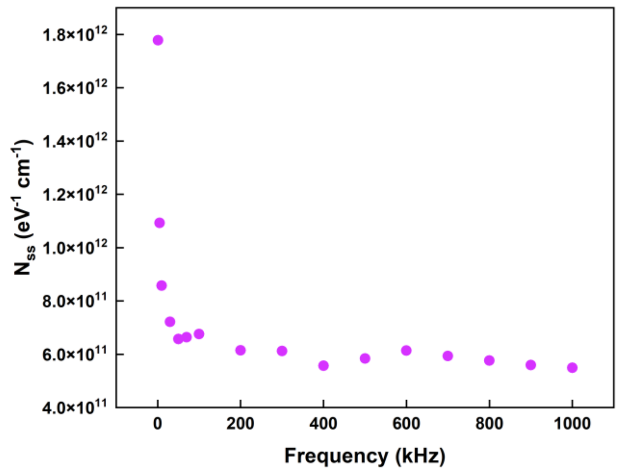

Figure 10: Characteristics of the Al/PyMIs/n-Si/Al Schottky diode based on a Hill-Coleman method

4. Conclusion

This study aims to investigate the diode by depositing the PyMIs organic interfacial layer between n-Si and Al using the spin coating process. The capacitance-voltage (*C-V*) and conductance-voltage (*G-V*) characteristics of the Al/PyMIs/n-Si/Al Schottky diode were measured throughout a frequency range of 1 kHz to 1 MHz. The capacitance values decreased, and the conductivity values raised within the frequency range of 1 kHz to 1 MHz. The distribution profiles of R_s and N_{ss} for the Al/PyMIs/n-Si/Al Schottky diode structure were determined through G-V and C-V measurements at wide frequencies. The series resistance (R_s) of the structure decreased with increasing voltage especially in the depletion region (-1.3 to -0.3 V), whereas increasing frequency caused a decrease in R_s values. The values of R_s for 2V decrease with increasing frequency and values varied from 1007 Ω at 5 kHz to 33.8 Ω at 1 MHz.

The significant number of interface states reported in low-frequency (5 kHz) capacitance-voltage measurements was considerably reduced by capacitance-voltage measurements up to 1 MHz. It has been shown that the N_{ss} values drop as the frequency increases. Specifically, the values ranged from 1.78×10^{12} eV^{-1} cm^{-2} at 1 kHz to 5.49×10^{11} eV^{-1} cm^{-2} at 1 MHz. This decline occurs because the charge carriers are unable to contribute to the capacity as the frequency increases. The results indicate that the manufactured Al/PyMIs/n-Si/Al Schottky diode has the potential to be used as a device in electronic applications.

References

[1] Nicollian E.H. and Brews J.R. MOS (metal oxide semiconductor) physics and technology. 2002: John Wiley & Sons.

[2] S.M. Sze K.K.N. Metal-Insulator-Semiconductor Capacitors. Physics of Semiconductor Devices, third ed. 2006, Hoboken, NJ, USA: John Wiley & Sons, Inc.

[3] Sharma B.L. Metal-semiconductor Schottky barrier junctions and their applications. 1984, US, Boston, MA: Springer.

[4] Kaplan N., Taşcı E., Emrullahoğlu M., et al. Analysis of illumination dependent electrical characteristics of α- styryl substituted BODIPY dye-based hybrid heterojunction. Journal of Materials Science: Materials in Electronics, 2021. 32(12): 16738-16747.

[5] Ulusoy M., Badali Y., Pirgholi-Givi G., Azizian-Kalandaragh Y., and Altındal Ş. The capacitance/conductance and surface state intensity characteristics of the Schottky structures with ruthenium dioxide-doped organic polymer interface. Synthetic Metals, 2023. 292: 117243.

[6] Yeşildağ A., Erdoğan M., Sevgili Ö., Çaldıran Z., and Orak İ. Optical and Electrical Properties of Pyrene–Imine Organic Interface Layer Based on p-Si. Journal of Electronic Materials, 2021. 50(11): 6448-6458.

[7] Kathiravan A., Sundaravel K., Jaccob M., et al. Pyrene Schiff Base: Photophysics, Aggregation Induced Emission, and Antimicrobial Properties. The Journal of Physical Chemistry B, 2014. 118(47): 13573-13581.

[8] Khan R.I., Ramu A., and Pitchumani K. Design and one-pot synthesis of a novel pyrene based fluorescent sensor for selective "turn on", naked eye detection of Ni2+ ions, and live cell imaging. Sensors and Actuators B: Chemical, 2018. 266: 429-437.

[9] Sayin S., Varol S.F., Merdan Z., and Eymur S. Synthesis of isoniazid substituted pyrene (PINHy), and investigation of its optical and electrochemical features as tunable/flexible OLEDs. Journal of Materials Science: Materials in Electronics, 2017. 28(17): 13094-13100.

[10] Taşçıoğlu İ., Tan S.O., and Altındal Ş. Frequency, voltage and illumination interaction with the electrical characteristics of the CdZnO interlayered Schottky structure. Journal of Materials Science: Materials in Electronics, 2019. 30(12): 11536-11541.

[11] Tataroğlu A., Altındal Ş., and Azizian-Kalandaragh Y. C-V-f and G/ω-V-f characteristics of Au/(In2O3-PVP)/n-Si (MPS) structure. Physica B: Condensed Matter, 2020. 582: 411996.

[12] Cavdar S., Demirolmez Y., Turan N., Koralay H., and Tuğluoğlu N. Analysis of voltage and frequency-dependent series resistance and interface states of Al/ZnCo2O4: Gelatin/n-Si diode. Journal of Materials Science: Materials in Electronics, 2022. 33(29): 22932-22940.

[13] Nicollian E.H. and Goetzberger A. MOS conductance technique for measuring surface state parameters. Applied Physics Letters, 1965. 7(8): 216-219.

[14] Cavas M., Farag A.A.M., Alahmed Z.A., and Yakuphanoglu F. Photosensors based on Ni-doped ZnO/p-Si junction prepared by sol-gel method. Journal of Electroceramics, 2013. 31(3): 298-308.

[15] Dökme İ., Yildiz D.E., and Altindal Ş. Illumination intensity effects on the dielectric properties of schottky devices with Co, Ni-doped PVA nanofibers as an interfacial layer. Advances in Polymer Technology, 2012. 31(1): 63-70.

[16] Nicollian E.H. and Goetzberger A. The Si-SiO_2 Interface — Electrical Properties as Determined by the Metal-Insulator-Silicon Conductance Technique. Bell System Technical Journal, 1967. 46(6): 1055-1133.

[17] Hill W.A. and Coleman C.C. A single-frequency approximation for interface-state density determination. Solid-State Electronics, 1980. 23(9): 987-993.

[18] Aydin S.B., Yildiz D.E., Çavuş H.K., and Şahingöz R. ALD TiO_2 thin film as dielectric for Al/p-Si Schottky diode. Bulletin of Materials Science, 2014. 37(7): 1563-1568.

[19] Tuğluoğlu N., Yüksel Ö.F., Karadeniz S., and Şafak H. Frequency dependent interface state properties of a Schottky device based on perylene-monoimide deposited on n-type silicon by spin coating technique. Materials Science in Semiconductor Processing, 2013. 16(3): 786-791.